

# UC Irvine

## UC Irvine Previously Published Works

### Title

Selecting optimal detector for temperature profiling in human skin using pulsed photothermal radiometry

### Permalink

<https://escholarship.org/uc/item/5b83w707>

### Authors

Majaron, B  
Milanič, M  
Choi, B  
[et al.](#)

### Publication Date

2005-06-01

### DOI

10.1051/jp4:2005125169

### Copyright Information

This work is made available under the terms of a Creative Commons Attribution License, available at <https://creativecommons.org/licenses/by/4.0/>

Peer reviewed

## Selecting optimal detector for temperature profiling in human skin using pulsed photothermal radiometry

B. Majaron<sup>1</sup>, M. Milanič<sup>1</sup>, B. Choi<sup>2</sup> and J.S. Nelson<sup>2</sup>

<sup>1</sup>*Jožef Stefan Institute, Jamova 39, 1000 Ljubljana, Slovenia*

<sup>2</sup>*Beckman Laser Institute, University of California, Irvine, CA 92612-1475, USA*

**Abstract.** We simulate temperature depth profiling in human skin using pulsed photothermal radiometry (PPTR). By taking into account blackbody emission characteristics, spectral variation of human skin IR absorption coefficient, detectivity of available radiation detectors, and shot noise, we compute realistic PPTR signals for a test temperature profile, representing a subsurface vascular lesion. Analysis of the reconstructed temperature profiles enables a performance comparison of quantum IR detectors utilizing different spectral acquisition bands. The results suggest that HgCdTe detector used in 6–10  $\mu\text{m}$  spectral band performs better than an InSb detector used at 4–5  $\mu\text{m}$ .

### 1. INTRODUCTION

In designing a pulsed photothermal radiometry (PPTR) setup for temperature depth profiling [1,2], application-specific details must be considered in addition to common detector characteristics such as detectivity, size and response time. While blackbody emission law determines radiometric signal amplitudes and background radiation shot noise, IR absorption coefficient value of skin ( $\mu_{\text{IR}}$ ) affects ill-posedness of the temperature profile reconstruction [2]. Spectral variation of  $\mu_{\text{IR}}(\lambda)$  may require narrowing of the acquisition band to ensure validity of the customary approximation of constant  $\mu_{\text{IR}}$  in data analysis [3]. This, in turn, reduces signal-to-noise ratio (SNR) in the radiometric signals, adversely affecting overall system performance.

We present a simulation study which takes into account all the elements mentioned above. Starting from an analytical temperature profile, resembling a laser-heated vascular lesion, we compute realistic PPTR signals for two radiation detectors (InSb, HgCdTe) and different spectral acquisition bands. From a quantitative analysis of the reconstructed temperature profiles we determine optimal acquisition bands for either detector and compare their performance.

### 2. METHODS

In PPTR, the laser-induced temperature profile  $\Delta T(z,0)$  can be reconstructed from measured radiative emission transient  $\Delta S_{\lambda}(t)$  by solving a Fredholm integral equation of the first kind [2]:

$$\Delta S_{\lambda}(t) = \int_0^{\infty} K_{\lambda}(z,t) \Delta T(z,0) dz . \quad (1)$$

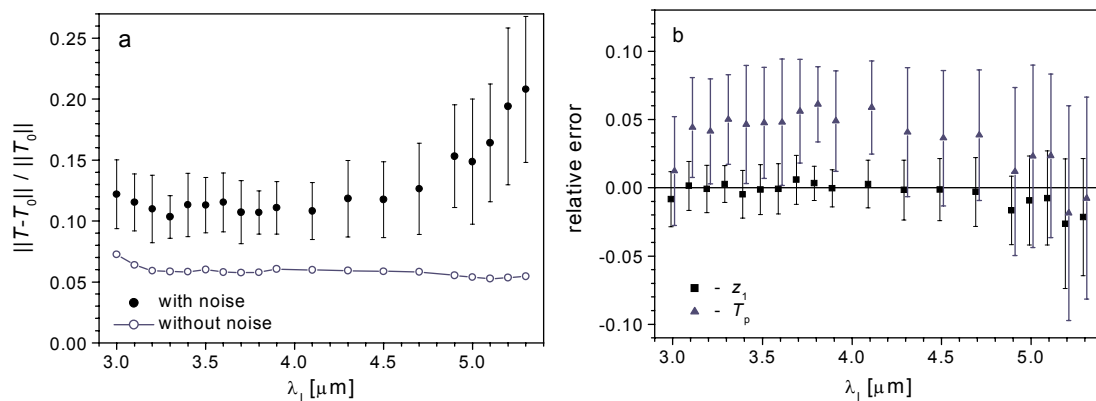
The involved kernel function  $K_{\lambda}(z,t)$  depends on detection wavelength  $\lambda$  through Planck's law of radiation and absorption coefficient of skin  $\mu_{\text{IR}}(\lambda)$  [2]. To simulate broad-band detection, we sum 100 contributions (1) within the detection band ( $\lambda_l$  to  $\lambda_h$ ), while taking into account spectral response of the detector  $R(\lambda)$ . This is equivalent to introducing an augmented kernel function [3,4].

As a test temperature profile, we use a hyper-Gaussian function  $\Delta T(z,0) = \Delta T_0 \exp[-2(z-z_0)^4/w^4]$  (with  $\Delta T_0 = 1$  K,  $z_0 = 300$   $\mu\text{m}$ ,  $w = 100$   $\mu\text{m}$ ), which has no sharp edges and thus serves as a suitable first model of a laser-heated subsurface vascular lesion in human skin [2,3]. (More complex and realistic initial temperature profiles will be included in a follow-up study.) Using a custom code in C++, signal values are computed at 1000 equidistant time points within a 1 s acquisition interval. Gaussian white noise is added to each signal point, with SNR computed by taking into account the detectors' spectral sensitivity, peak detectivity ( $D^*$ ), area ( $A$ ), collecting power of suitable optics, and radiometric signal shot noise [4]. For each example, 30 signal vectors  $\mathbf{S}$  are simulated by adding noise computed using different random-number generator seeds, allowing for statistical evaluation of the influence of noise on the reconstruction results.

Reconstruction of  $\Delta T(z,0)$  from  $\mathbf{S}$  is a severely ill-posed inverse problem without a unique solution. We solve it by iterative minimization of the quadratic residual norm  $\|\mathbf{K}\cdot\mathbf{T}^{(n)} - \mathbf{S}\|$ , with vector  $\mathbf{T}$  representing temperature values at 100 equidistant points within the most superficial millimeter of "skin". To that end, we implemented a conjugate-gradient algorithm with nonnegativity constraint [2] in a custom code within the MatLab programming environment. The customary approximation of spectrally constant absorption coefficient  $\mu_{\text{eff}}$  is applied in the profile reconstruction process. Determination of the optimal  $\mu_{\text{eff}}$  for each spectral band and detector is a nontrivial task [3,4]. Due to space limitations, it will be described in a follow-up publication.

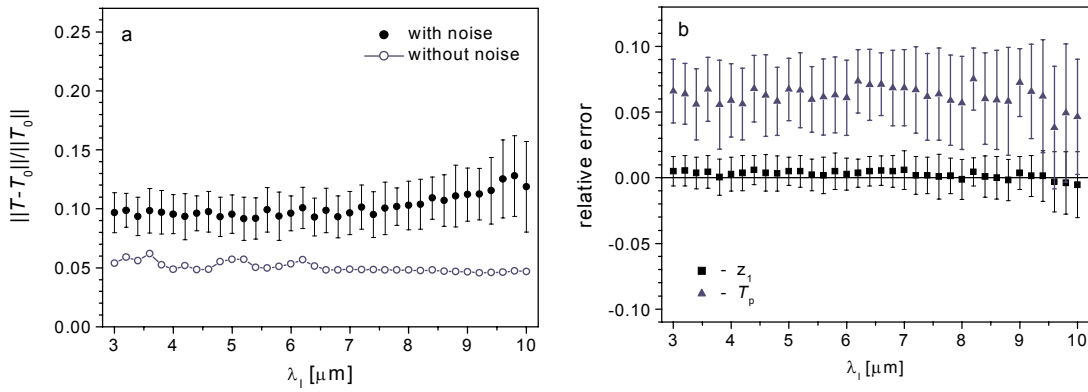
### 3. RESULTS

Figure 1 presents the results for a typical InSb detector with peak sensitivity at  $\lambda_p = 5.3$   $\mu\text{m}$  ( $D^* = 1.5 \times 10^{11}$   $\text{cm (Hz)}^{1/2}/\text{W}$ ,  $A = 0.78$   $\text{mm}^2$ ). The upper detection band limit is set to  $\lambda_h = 5.5$   $\mu\text{m}$ , where the detector sensitivity drops to 10%, and  $\lambda_l$  is varied between 3.0 and 5.3  $\mu\text{m}$ .



**Figure 1.** Analysis of reconstruction results for the InSb detector. (a) Quadratic norm of the difference between the reconstructed and actual temperature profile vectors, relative to quadratic norm of the latter. (b) Relative error of the superficial edge depth  $z_1$  (squares) and of the peak temperature  $T_p$  (triangles) in the reconstructed profile. Solid symbols and error bars represent average values and standard deviations from 30 runs with realistic SNR.

Figure 2 shows the results for a typical HgCdTe detector ( $D^* = 4 \times 10^{10}$   $\text{cm (Hz)}^{1/2}/\text{W}$ ,  $A = 1.0$   $\text{mm}^2$ ) with sensitivity peak at  $\lambda_p = 10$   $\mu\text{m}$  (dropping to 10% at  $\lambda_h = 12$   $\mu\text{m}$ ). The lower detection limit  $\lambda_l$  is varied between 3.0 and 10  $\mu\text{m}$ .



**Figure 2.** Analysis of reconstruction results for the HgCdTe detector. (See Fig. 1 for details).

From the results, we deduce that the optimal  $\lambda_1$  is 4.1  $\mu\text{m}$  for InSb, and around 6  $\mu\text{m}$  for HgCdTe detector. The corresponding signal and noise levels (in A), for our test temperature profile are listed in Table 1. Comparison of the corresponding temperature profile reconstructions (summarized in last two columns) shows that with the HgCdTe detector, the depth of half-maximum point of the profile ( $z_1$ ) can be assessed more reliably, and the reconstructed profile deviates less from the actual one.

**Table 1.** Optimal acquisition band ( $\lambda_l - \lambda_h$ ), effective absorption coefficient value ( $\mu_{\text{eff}}$ ), signal ( $S$ ) and combined noise level ( $N$ ), and resulting SNR for the two detectors under consideration. Reconstructed temperature profiles are evaluated in terms of depth at half-maximum point ( $z_1$ ; actual profile has  $z_1 = 0.223$  mm) and quadratic norm of the difference between the reconstructed and actual profile, relative to the norm of the actual profile vector  $T_0$ .

Detector	Spectral band	$\mu_{\text{eff}}$ [ $\text{mm}^{-1}$ ]	$S$ [A]	$N$ [A]	SNR	$z_1$ [mm]	$\ T - T_0\  / \ T_0\ $
InSb	4.1 – 5.6 $\mu\text{m}$	$23.7 \pm 1.1$	$9.26 \times 10^{-9}$	$5.0 \times 10^{-11}$	221	$0.224 \pm 0.003$	0.108
HgCdTe	6.0 – 12 $\mu\text{m}$	$56.6 \pm 0.4$	$8.66 \times 10^{-7}$	$2.1 \times 10^{-9}$	437	$0.224 \pm 0.002$	0.096

#### 4. CONCLUSION

For the discussed application, exploring the 6–10  $\mu\text{m}$  acquisition band with a HgCdTe detector offers better performance than InSb detector used in the customary 3–5  $\mu\text{m}$  band.

#### References

[1] Jacques S.L., Nelson J.S., Wright W.H., Milner T.E., *Appl. Opt.* **32** (1993) 2439-2446.  
 [2] Milner T.E., Goodman D.M., Tanenbaum B.S., Nelson J.S., *J. Opt. Soc. Am. A* **12** (1995) 1479-88.  
 [3] Majaron B., Verkruysse W., Tanenbaum B.S., Milner T.E., Nelson J.S., *Phys. Med. Biol.* **47** (2002) 1929-1946.  
 [4] Majaron B., Milanič M., Choi B., Nelson J.S., *Proc. SPIE* vol. **5318** (2004) 121-132.